Theory and Numerics for a Semilinear Elliptic PDE, with an Application in the Theory of Pseudoplastic Fluids

Van Emden Henson*
Department of Mathematics
Naval Postgraduate School

Aihua W. Shaker
Department of Mathematics
Air Force Institute of Technology

Abstract

In this work we provide a survey of the existence, uniqueness, and analyticity of the solutions for the problem

$$\Delta u + p(x)u^{-\gamma} = 0, \quad x \in \Omega \subseteq R^n, \quad n \geq 1.$$

We establish numerical solutions in one- and two-dimensional bounded regions using multigrid methods. Numerical examples are provided that demonstrate the necessity and/or sufficiency of some the conditions in the existence and uniquness theorems.

AMS Subject Classification: 35J25, 35J60, 65N55
Keywords: semilinear, elliptic, multigrid, FAS, pseudoplastic flow

1 Introduction

We study the singular semilinear elliptic boundary value problem

$$\begin{array}{l} \Delta u + p(x)u^{-\gamma} = 0, \quad x \in \Omega \subseteq R^n, \\ u \mid_{\partial\Omega} = 0, \end{array} \tag{1}$$

whose importance in scientific applications has been widely recognized [15]. In particular, in the case $n = 1$, the problem arises in the study of boundary layer equations for a class of non-Newtonian fluids, namely pseudoplastic fluids, under the classical conditions for a steady flow over a semi-infinite flat plate [3]. Considered in the context of partial differential equations ($n > 1$), the above equation has been

*This work was supported in part by the the Naval Postgraduate School Research Council under grant No. ZZ867-ZZ899/5986

the subject of much study. (See, for example, [4], [5], [6], [7], [8], [13] and their references.) Kusano and Swanson [5] consider (1) in which $0 < \gamma < 1$, $\Omega = R^n$, and prove that if $p \in C^{\alpha}_{loc}(R^n)$, $0 < \alpha < 1$, $p(x) > 0$ on $R^n \backslash \{0\}$, $\frac{p(x)}{\phi(|x|)}$ is bounded above and below where $\phi(t) = \max_{|x|=t} p(x)$, and

$$\int_0^{\infty} t^{n-1+\gamma(n-2)} \phi(t) dt < \infty, \tag{2}$$

then (1) has a $C^{2+\alpha}_{loc}(R^n)$ positive solution on R^n. Edelson [4] studies (1) under essentially the same conditions as in [7] but bases his work on classical integral operator equations in R^n instead of the barrier method employed in [5]. This provides no additional information on the existence of positive solutions of (1), but it does give a context in which higher order equations similar to (1) may be studied. Shaker [13] fills out the work of [4] and [5] by establishing existence for all $\gamma > 0$. Lair and Shaker [7] extend all of these results by proving the existence of a positive $C^{2+\alpha}_{loc}(R^n)$ solution for more general p. In particular, the function p is allowed to be zero on large parts of R^n. However, zeros of p must be "surrounded" by a region where $p(x) > 0$. Also in [7], inequality (2) is replaced by the weaker condition

$$\int_0^{\infty} t\phi(t) dt < \infty. \tag{3}$$

Furthermore, Lair and Shaker show that condition (3) is nearly optimal.

For bounded Ω, Lazer and McKenna [6] use the standard upper-lower solution technique to prove that if p is a strictly positive $C^{\alpha}(\bar{\Omega})$ function, then (1) has a unique positive $C^{2+\alpha}_{loc}(\Omega)$ solution which is continuous on $\bar{\Omega}$. Pino [11] provided a global estimate for the gradient of the solution and establishes an existence result for $p \in L^{\infty}(\Omega)$. Lair and Shaker [8] consider the more general equation

$$\begin{array}{ll} \Delta u + p(x) f(u) = 0, & x \in \Omega \subseteq R^n, \\ u = 0, & x \in \partial\Omega, \end{array} \tag{4}$$

where $f(u)$ satisfies assumptions

$$\begin{aligned} f'(s) &\leq 0 && (5) \\ f(s) &> 0, \text{ if } s > 0 && (6) \\ \int_0^{\epsilon} f(s) &< \infty \text{ for some } \epsilon > 0, && (7) \end{aligned}$$

and show that that (4) has a unique positive weak solution in $H^1_o(\Omega)$, provided p is a nontrivial, nonnegative $L^2(\Omega)$ function.

The purpose of this paper is to provide a survey of the theory governing solutions to (1). Additionally, through numerical solutions we analyze the necessity and/or sufficiency of a few representative theorems, provide insights for further study of this problem.

2 Some analytical results

In this section we state three theorems regarding solutions of (1) and (4) in bounded domains. Our numerical experiments in Section 4 are designed, in part, to illustrate the theoretical properties of the solutions these theorems delineate.

Theorem 1 *(Lazer-McKenna [6]). Problem (1) has a unique positive solution $u(x)$ in Ω with $u \in C^{2+\alpha}(\Omega) \cap (\bar{\Omega})$, where Ω is a bounded domain in R^n, $n \geq 1$. Furthermore let ϕ be an eigenfunction corresponding to the smallest eigenvalue λ_1 of the problem*

$$\begin{aligned} \Delta\phi + \lambda\phi = 0, \quad x \in \Omega \\ \phi \mid_{\partial\Omega} = 0 \end{aligned}$$

such that $\phi_1(x) > 0$, $x \in \Omega$ and $\lambda > 1$. Then there exists a unique $b_1, b_2 > 0$ such that

$$b_1\phi_1^{2/(1+\lambda)} \leq u \leq b_2\phi_1^{2/(1+\lambda)}$$

on $\bar{\Omega}$.

Theorem 2 *(Lair-Shaker [8]). Problem (4) has a unique positive solution in $C_{loc}^{2+\alpha}(\Omega)$ if p is a nontrivial, nonnegative $C_{loc}^{\alpha}(\Omega)$ function, f satisfies (5) and (6), and $\Omega = B(x_o, R)$, $R < \infty$.*

Theorem 3 *(Lair-Shaker [8]). If p is a nontrivial, nonnegative $L^2(\Omega)$ function, where Ω is a bounded domain in R^n and f satisfies (5)-(7), then problem (4) has a unique weak positive solution $u(x) \in H_o^1(\Omega)$ in the sense that*

$$\int_{\Omega} (\nabla u \cdot \nabla v - p(x)f(u)v)dx = 0, \quad \forall v \in H_o^1(\Omega). \tag{8}$$

Note that for the case when $f(u) = u^{-\gamma}$ (7) requires that $0 < \gamma < 1$.

2.1 Methods

In general there are two methods that are commonly used in proving existence and uniqueness of solutions for equations of type (1), namely *Schauder's fixed point thoerem* and *Barrier Methods.* Since the former is standard we elaborate here only on the latter.

Let Ω be a smoothly bounded domain in R^n. $\phi(x)$ is said to be an upper (lower) solution of the problem

$$\begin{aligned} \Delta u + f(x,u) = 0, \quad x \in \Omega \\ u \mid_{\partial\Omega} = 0 \end{aligned} \tag{9}$$

if $\Delta\phi + f(x,\phi) \leq 0$, $x \in \Omega$, $\phi(x) \geq 0$ $x \in \partial\Omega$ ($\phi + f(x,\phi) \geq 0$, $x \in \Omega$, $\phi(x) \leq 0$ $x \in \partial\Omega$).

Theorem 4 *(Sattinger [12]). Let ϕ_1 be an upper solution and ϕ_2 be a lower solution of (9), and let f be locally Hölder continuous in Ω. If $\phi_1(x) \geq \phi_2(x)$ in Ω, then (9) has a solution u such that $\phi_2(x) \leq u(x) \leq \phi_1(x)$, $x \in \bar{\Omega}$.*

In the case when $\Omega = R^n$ we say ϕ is an upper (lower) solution of

$$\Delta u + f(x,u) = 0 \tag{10}$$

if $\Delta\phi + f(x,\phi) \le 0$ $x \in R^n$ (for lower solution, $\Delta\phi + f(x,\phi) \ge 0$).

Theorem 5 *(Ni [10]). Let ϕ_1 and ϕ_2 be an upper and a lower solution of equation (10), such that $\phi_1 \ge \phi_2$ $x \in R^n$. If f is locally Hölder continuous in x and locally Lipschitz continuous in u, then (10) has a solution u with $\phi_2(x) \le u(x) \le \phi_1(x)$, $x \in R^n$.*

An Example.
Consider the problem

$$\begin{array}{ll} u'' + \lambda u - u^3 = 0, & x \in (0,\pi) \\ u = 0, & x = 0, \pi, \end{array}$$

where $\lambda > 1$. It is easy to show that $\phi_1(x) = Rx^{1/2}$ for some R large is an upper solution, and $\phi_2(x) = \epsilon \sin x$ for some ϵ small is a lower solution of this problem. Clearly $\phi_1(x) \ge \phi_2(x)$ for $x \in [0,\pi]$. Thus by the above theorem there is a solution $u(x)$ such that $\epsilon \sin x \le u(x) \le Rx^{\frac{1}{2}}$, $x \in [0,\pi]$. Since the problem is homogeneous we conclude that the problem has at least three solutions, namely, u, $-u$ and the trivial solution.

3 An Application for $n = 1$

For $n = 1$ equation (1) arises in the study of pseudoplastic fluids [3]. A non-Newtonian fluid is called *pseudoplastic* if the shear stress τ and the strain rate $\dfrac{\partial u}{\partial y}$ are related as

$$|\tau| = k\left|\frac{\partial u}{\partial y}\right|^{\alpha}, \quad 0 < \alpha < 1$$

where k is a positive constant. That is, the absolute value of the shear stress increases with respect to the absolute value of the strain rate less than linearly. Here we show that through a series of transformations the boundary layer equations for the class of pseudoplastic fluids under the classical conditions for a steady flow over a semi-infinite flat plate can be generalized into the well-known Blasius problem

$$f''' + ff' = 0,$$

$$f(0) = f'(0) = 0, \quad f'(\infty) = 1$$

for the shear function, which arises from the standard Newtonian fluid case.

Consider a two-dimensional incompressible flow of low viscosity along a plane wall. We denote by $\vec{v} = (u,v)$ the fluid velocity in the boundary layer and $u_\infty(x)$ in the main stream. Since there is no velocity on the wall ($y = 0$) and the fluid takes the velocity of the main stream $u_\infty(x)$ outside the boundary layer, we see that $\dfrac{\partial u}{\partial y}$ is large near the wall which causes a significant transfer of momentum in the x direction.

The boundary layer equations for this model include a continuity equations and a momentum equation in the x direction.

$$\begin{gathered}\frac{\partial u}{\partial x}+\frac{\partial u}{\partial y}=0\\ u\frac{\partial u}{\partial x}+v\frac{\partial u}{\partial y}=\frac{1}{\rho}\frac{\partial \tau_{xy}}{\partial y}\end{gathered}\tag{11}$$

with boundary conditions

$$\begin{gathered}u(x,0)=v(x,0)=0,\\ u(x,\infty)=u_\infty(x)\end{gathered}$$

where $\tau_{xy}=K\left|\frac{\partial u}{\partial y}\right|^\alpha$ is the shear stress.

Note that (11) has 2 coupled equations in 3 dependent variables, u, v, and τ_{xy}. To reduce it to a single higher-order equation in only 1 dependent variable, we introduce the Lagrange stream function $\Phi(x,y)$ such that

$$u=\frac{\partial \Phi}{\partial y},\quad v=-\frac{\partial \Phi}{\partial x}.$$

Then the momentum equation becomes

$$\frac{\partial \Phi}{\partial y}\cdot\frac{\partial^2\Phi}{\partial x\partial y}-\frac{\partial \Phi}{\partial x}\cdot\frac{\partial^2\Phi}{\partial y^2}=\nu\frac{\partial}{\partial y}\left(\frac{\partial^2\Phi}{\partial y^2}\right)^\alpha.\tag{12}$$

where $\nu=\frac{K}{\rho}$, while the continuity equation is clearly satisfied by Φ.

Let $f=\frac{a\Phi}{\sqrt{u_\infty \nu x}}$; $\eta=by\sqrt{\frac{u_\infty}{\nu x}}$, for some a,b. Then (12) becomes

$$f'''+f(f'')^{2-\alpha}=0\tag{13}$$

with

$$\begin{aligned}&f(0)=f'(0)=0\\ &f'(\infty)=1\end{aligned}$$

where $f=f(\eta)$. (Observe that if $\alpha=1$ (13) is the well-known Blasius equation.) Employing the Crocco-like transformation

$$u=f'(\eta),\quad g(u)=u'=f''(\eta)$$

(13) becomes

$$g^\alpha g''+(\alpha-1)g^{\alpha-1}(g')^2+u=0$$

with $g'(0)=0$, $g(1)=0$, where $g=g(u)$. Finally the transformation $G=g^\alpha$ leads to the singular boundary value problem

$$\begin{aligned}&G''+\alpha u G^{-1/\alpha}=0,\quad 0<u,\alpha<1,\\ &G'(0)=G(1)=0\end{aligned}$$

of the form (1) with $\lambda=\frac{1}{\alpha}$, $u=x$, $p=\frac{x}{\lambda}$.

4 Numerical solutions

In this section we present some numerical results for solving the problem

$$\begin{aligned} \Delta u + p(x)\, u^{-\gamma} &= 0 \qquad x \in \Omega \\ u(x) &= 0 \qquad x \in \partial\Omega. \end{aligned}$$

Specifically, we describe a multigrid $V-cycle$ method using the nonlinear Newton-Gauss-Seidel iteration as a smoother (relaxation method). We have implemented this method for both the one- and two-dimensional cases, using (respectively) the unit interval and the unit square for Ω. In each case we use a straightforward finite-difference discretization, employing the standard second-order difference approximation for the second derivative operator. For the one-dimensional problem we define the grid of $(N+1)$ points $x_k = jh$, for $k = 0, 1, \ldots N$, where h is the mesh parameter $1/N$. The second derivative operator is then approximated by

$$\left.\frac{d^2u}{dx^2}\right|_{x_k} \approx \frac{u_{k-1} - 2u_k + u_{k+1}}{h^2},$$

where u_k approximates $u(x_k)$. For the non-linear term $p(x)u(x)^{-\gamma}$ we use the nodal values, $p_k\, u_k^{-\gamma}$. Since $u_0 = u_N = 0$, this results in the non-linear system of equations

$$\frac{1}{h^2}\begin{bmatrix} -2 & 1 & & & & \\ 1 & -2 & 1 & & & \\ & \ddots & \ddots & \ddots & & \\ & & & 1 & -2 & 1 \\ & & & & 1 & -2 \end{bmatrix} \begin{bmatrix} u_1 \\ u_2 \\ \vdots \\ u_{N-2} \\ u_{N-1} \end{bmatrix} + \begin{bmatrix} p_1\, u_1^{-\gamma} \\ p_2\, u_2^{-\gamma} \\ \vdots \\ p_{N-2}\, u_{N-2}^{-\gamma} \\ p_{N-1}\, u_{N-1}^{-\gamma} \end{bmatrix} = \begin{bmatrix} 0 \\ 0 \\ 0 \\ \vdots \\ 0 \end{bmatrix}. \tag{14}$$

Letting u represent the vector of unknowns, we may write the system as $Au + g(u) = 0$, where A is the tridiagonal matrix and g is the non-linear vector function.

For the two-dimensional case we take the tensor product of the $(N+1)$-point grid in the x direction with an identical $(N+1)$-point grid in the y direction, yielding an $(N+1)^2$-point regular grid covering the unit square. The difference operator for the two-dimensional problem is

$$\left.\left(\frac{\partial^2 u}{\partial x^2} + \frac{\partial^2 u}{\partial y^2}\right)\right|_{x_{j,k}} \approx \frac{u_{j-1,k} - 2u_{j,k} + u_{j+1,k}}{h^2} + \frac{u_{j,k-1} - 2u_{j,k} + u_{j,k+1}}{h^2}.$$

Numbering the unknowns lexicographically by lines of constant y, we obtain the nonlinear system

$$\begin{bmatrix} A & B & & & & \\ B & A & B & & & \\ & \ddots & \ddots & \ddots & & \\ & & & B & A & B \\ & & & & B & A \end{bmatrix} \begin{bmatrix} u_1 \\ u_2 \\ \vdots \\ u_{N-2} \\ u_{N-1} \end{bmatrix} + \begin{bmatrix} w_1 \\ w_2 \\ \vdots \\ w_{N-2} \\ w_{N-1} \end{bmatrix} = \begin{bmatrix} 0 \\ 0 \\ 0 \\ \vdots \\ 0 \end{bmatrix} \tag{15}$$

where u_j denotes the $(N-1)$-length vector of unknowns $u_{j,k}$ for $k = 1, 2, \ldots, N-1$ corresponding to the j^{th} grid-line in the y direction, A is the $(N-1) \times (N-1)$

matrix

$$A = \frac{1}{h^2}\begin{bmatrix} -4 & 1 & & & & \\ 1 & -4 & 1 & & & \\ & \ddots & \ddots & \ddots & & \\ & & & 1 & -4 & 1 \\ & & & & 1 & -4 \end{bmatrix},$$

and B is $-1/h^2$ times the identity. The $(N-1)$-length vectors w_j contain the non-linear entries $p_{j,k}\, u_{j,k}^{-\gamma}$, for $k = 1, 2, \ldots, N-1$. We may write the system as $Hu + g(u) = 0$, where H is the block tri-diagonal matrix and g is the non-linear vector function containing the w_j's.

In either the one-dimensional or two-dimensional case we may write the system in the form

$$F(u) = 0, \tag{16}$$

where F is the nonlinear operator $Au + g(u)$ or $Hu + g(u)$, as appropriate.

4.1 Multigrid methods

Multigrid methods may be thought of as accelerators for iterative "relaxation" methods. Letting u^* represent the exact solution, u the current approximation, and $e \equiv u - u^*$ the *error*, then iterative methods can be written in the form $e \leftarrow Pe$ where P is the *relaxation matrix* or *error propagation matrix.* At the heart of multigrid is the coarse-grid correction [2]. Many common iterative relaxation methods for solving a linear problem $Au = f$ have the property that the relaxation effectively eliminates the high-frequency (oscillatory) components of the error e but leave the low frequency (smooth) components essentially unaffected. However, because the error is smooth after the relaxation, it may be represented accurately on a coarser grid (i.e., one with fewer, more widely-spaced gridpoints), on which it also appears (relatively) more oscillatory. Relaxation on this coarser grid then eliminates the oscillatory components of the coarse-grid error, which cannot be eliminated on the fine grid.

Denoting fine-grid vectors with the superscript h and their coarse-grid counterparts with the superscript $2h$, the coarse-grid correction for a linear problem may be written as

$$u^h \leftarrow P^\nu u^h + I_{2h}^h (A^{2h})^{-1} I_h^{2h} (f^h - A^h P^\nu u^h)$$

where P is the relaxation matrix, ν is the number of relaxations performed on the fine grid, I_{2h}^h is a *prolongation* or *interpolation* matrix mapping coarse-grid vectors to the fine grid, I_h^{2h} is a *restriction* matrix mapping fine-grid vectors to the coarse grid, and A^{2h} is a coarse-grid version of the original matrix A. A crucial feature is that on the coarse grid Ω^{2h}, the problem to be solved is the *residual* equation

$$Ae = r, \tag{17}$$

where the residual is defined $r = f - Au$ and e is the error. That is,

$$Ae = A(u^* - u) = f - Au = r.$$

4.2 Full Approximation Scheme (FAS)

For *nonlinear* problems the residual equation (17) doesn't hold. Instead, we write the nonlinear equivalent of the residual equation,

$$F(u+e) \;-\; F(u) \;=\; r.$$

This equation is to be solved on the coarse grid, so we write

$$F^{2h}(I_h^{2h}u^h + e^{2h}) \;-\; F^{2h}(I_h^{2h}u^h) \;=\; I_h^{2h}(f^h - F^h(u^h)), \tag{18}$$

or

$$F^{2h}(u^{2h}) \;=\; I_h^{2h}(f^h - F^h(u^h)) + F^{2h}(I_h^{2h}).$$

The coarse-grid correction is then performed by solving (18) for $u^{2h} \;=\; I_h^{2h}u^h + e^{2h}$, and then making the correction $u^h \leftarrow u^h + I_{2h}^h(u^{2h} - I_h^{2h}u^h)$. This gives the Full Approximation Scheme [1]

$$u^h \leftarrow P^\nu(u^h) + I_{2h}^h((F^{2h})^{-1}(I_h^{2h}(f^h - F^h(P^\nu(u^h))) + F^{2h}(I_h^{2h}P^\nu(u^h))) - I_h^{2h}P^\nu(u^h)),$$

where P is a nonlinear relaxation scheme.

For both the linear and nonlinear problems, the solution of the coarse-grid problem is computed using the same coarse-grid correction scheme as is being employed to solve the fine-grid problem. This leads to the multigrid *V-cycle* scheme, which (for the nonlinear problem using *FAS*) is described recursively as follows.

$$u^h \leftarrow\; FASV^h(u^h, f^h, \nu_1, \nu_2)$$

1. Perform ν_1 non-linear relaxation sweeps times on $F^h(u^h) = f^h$ with initial guess u^h.
2. If Ω^h is the coarsest grid, then go to 4. Else:
   $f^{2h} = I_h^{2h}(f^h - F^h(u^h)) + F^{2h}(I_h^{2h}u^h)$
   $u^{2h} \leftarrow 0$
   $u^{2h} \leftarrow FASV^{2h}(u^{2h}, f^{2h}, \nu_1, \nu_2)$.
3. Correct $u^h \leftarrow u^h \;+\; I_{2h}^h(u^{2h} - I_h^{2h}u^h)$.
4. Perform ν_2 non-linear relaxation sweeps times on $F^h(u^h) = f^h$ with initial guess u^h.

4.3 Numerical results for multigrid methods

We implement the $FASV$ using Newton-Jacobi and Red-black Newton-Gauss-Seidel iteration schemes for this study. These are easily described for the one-dimensional case, in which the general form of each equation in the system is

$$u_{k-1} - 2u_k + u_{k+1} + h^2 p_k u_k^{-\gamma} = 0. \tag{19}$$

Formally, Newton-Jacobi nonlinear relaxation consists of solving (19), for u_k, using Newton's method, while holding the other entries of the vector u unchanged. The entire vector u is then updated with new values after the complete set of u_k's has been determined. Newton Gauss-Seidel is the same process except that the new values of u_k are immediately employed in the computation of the remaining elements of u, while the designation "red-black" is used to indicate the order in which the individual entries of u are updated. In practice we do not *solve* equation (19); rather, we perform one or two steps of Newton's method, moving the value of u_k toward its solution.

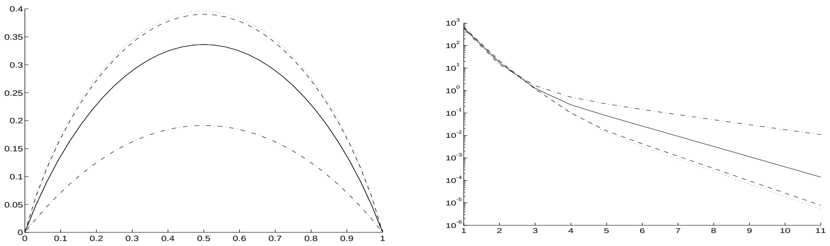

Figure 1: LEFT: *A sequence of lower solutions for* $\Delta u + p(x)u^{-\gamma} = 0$, *generated by solving* $\Delta u + p(x)(u+d)^{-\gamma} = 0$ *using* $p(x) \equiv 1$, *and* $\gamma = 1$. RIGHT: *Residual norm of computed solution, plotted as against the number of V-cycles. On both plots the values of* d *used are* $d = 0.5$ *(dash-dot curve),* $d = 0.1$ *(solid curve),* $d = 0.01$ *(dashed curve), and* $d = 0.0015$ *(dotted curve).*

4.3.1 The one-dimensional case

We first examine an experiment designed to demonstrate numerically the barrier method used in the theoretical results developed above. Specifically, the *FAS V-cycle* method is employed, beginning with a random initial guess, to solve the one-dimensional problem

$$\Delta u + p(x)(u+d)^{-\gamma} \; = \; 0,$$

where $p(x) = 1$ and d is a small positive number. The parameter d is used to bound $u + d$ away from zero, so that $(u+d)^{-\gamma}$ remains finite. The function u is then a lower solution to the problem

$$\Delta u + p(x)u^{-\gamma} \; = \; 0.$$

The relaxation method employed is Red-Black Newton-Gauss-Seidel. By solving this problem for a sequence of decreasing values of d, a succession of lower solutions is produced, increasing toward the solution of the parameter-free ($d = 0$) problem, whose solution we ultimately seek. The succession of lower solutions is shown in the left graph of Figure 1.

Useful information about the performance of the numerical method is obtained by examining the norm of the residual, $||\Delta u + p(x)(u+d)^{-\gamma}||$. The logarithm of this quantity is plotted, as a function of the number of V-cycles, for each of the d-values, in the right graph of Figure 1. The rate of convergence is obtained by examining the ratio of residual norm after a V-cycle to the residual norm before the V-cycle. For each value of d the convergence ratios are quite good, getting slightly better as d decreases. In the best case, for $d = 0.0015$, the convergence ratio is extremely good through the first few V-cycles (0.03, 0.06, 0.08) and increases thereafter before steadying at 0.27, which is not atypical for nonlinear problems.

We next consider the effect of altering γ. For this we examine the problem $\Delta u + p(x)u^{-\gamma} = 0$, using $p(x) = x$ and $\gamma = 1, 2, 4,\ 5$, and 6. The solution curves are plotted in Figure 2. The solutions are characterized by greater curvature as γ increases. Along with this, the numerical methods require more effort to achieve

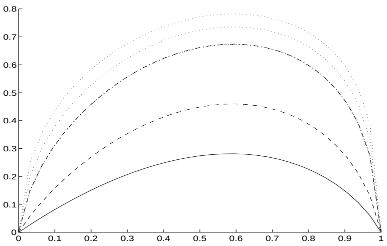

Figure 2: *Solutions for $\Delta u + p(x)u^{-\gamma} = 0$, for $\gamma = 1, 2, 4, 5,$ and 6 (bottom to top). Note the increase in curvature as γ increases.*

an acceptable solution, in the sense that more V-cycles are required to bring the residual norms down. This should not be surprising considering the stronger nonlinearity with greater γ, and that near the boundaries the Laplacian must get larger (more negative) to counter the tendency for the nonlinear term to blow up. The asymptotic convergence ratios remain good - averaging 0.27 to 0.25, but the initial residuals for large γ are sufficiently large that more V-cycles are required to obtain reasonable solutions.

4.3.2 The two-dimensional case

Several experiments are utilized to demonstrate the performance of the numerical method on two-dimensional problems. Several different choices for γ and $p(x, y)$ are used. The first set of experiments are displayed in Figure 3. Solutions are displayed for $p(x, y) = 1$, $p(x, y) = x$, $p(x, y) = x^2y$, and $p(x, y) = x/y$. In all cases $\gamma = 1$. The effect on the solution of the increasing complexity (and stronger nonlinearity) of the coefficient term $p(x, y)$. As is easily seen from the convergence curves, however, the function $p(x, y)$ has remarkably little effect on the convergence properties of the method. Table I gives some quantitative information regarding the performance of the method, comparing convergence ratios for various choices of functions $p(x, y)$ and parameters γ. The results shown are obtained using the Red-black Newton-Gauss-Seidel relaxation. We find that for this problem we are able to obtain convergence ratios that are similar to those obtained on the linear elliptic model problems for which multigrid is best known ([2], [9], [14]). It may be seen that in the presence of stronger nonlinearity ($\gamma = 8$) that convergence factor is somewhat higher. In addition, the random initial guesses have larger initial residuals in these cases, and these two facts conspire so that convergence to a given residual size often requires considerably more V-cycles than in the cases with weaker nonlinearity.

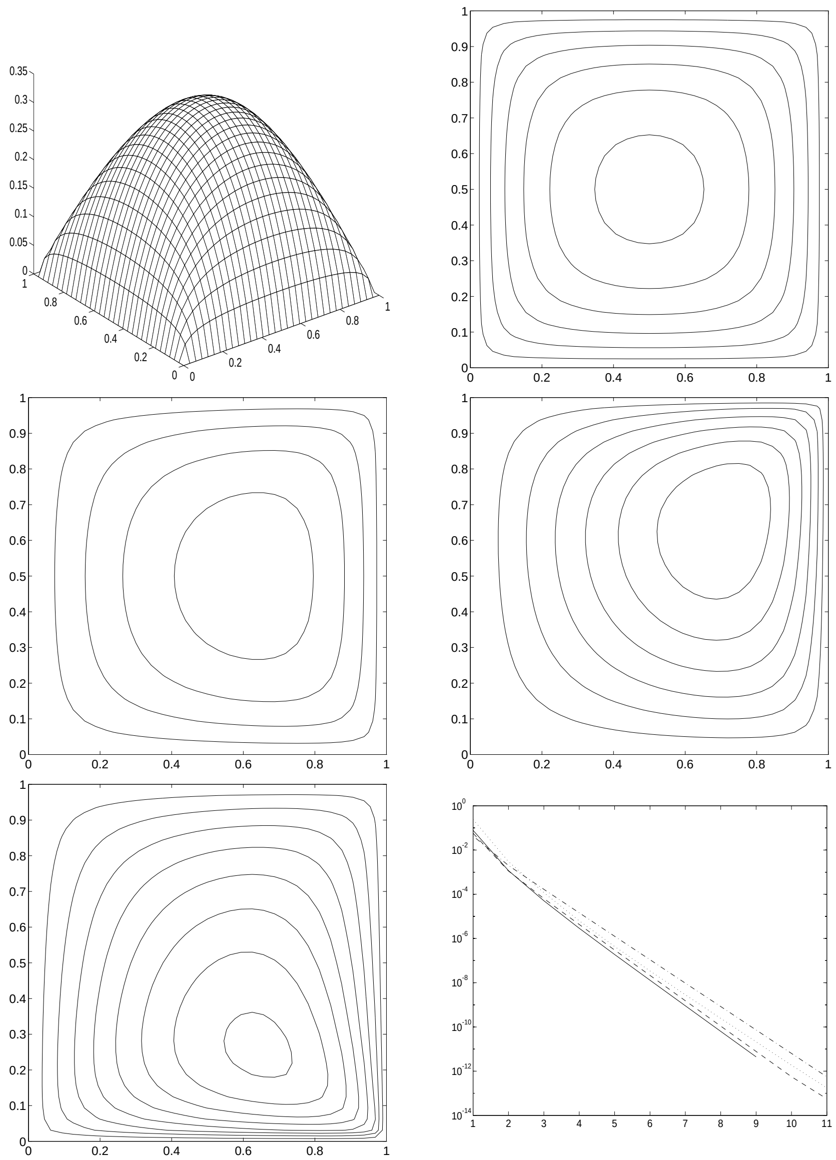

Figure 3: *Solutions for* $\Delta u + p(x,y)u^{-\gamma} = 0$. TOP LEFT: *Surface plot of solution for* $p(x,y) \equiv 1$. TOP RIGHT: *Contour plot of solution using* $p(x,y) \equiv 1$. MIDDLE LEFT: *Contour plot of solution with* $p(x,y) = x$. MIDDLE RIGHT: *Contour plot of solution with* $p(x,y) = x^2y$. BOTTOM LEFT: *Contour plot of solution with* $p(x,y) = x/y$. BOTTOM RIGHT: *Logarithms of ratios of convergence, plotted as functions of the number of V-cycles, for* $p(x,y) \equiv 1$ *(solid curve),* $p(x,y) = x$ *(dashed curve),* $p(x,y) = x^2y$ *(dash-dotted curve), and* $p(x,y) = x/y$ *(dotted curve).*

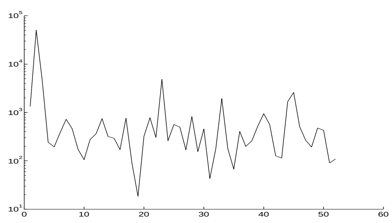

Figure 4: *The logarithm of the residual norm, as a function of the number of V-cycles, for the case $p(x,y) = x - 1/2$. The method fails to converge in this case.*

$p(x,y)$	γ	Fine-grid size	Average V-cycle convergence factor
$2xy$	2	63×63	0.051
	5		0.050
	8		0.078
x/y	2	63×63	0.059
	2		0.060
	8		0.086

Table I. *Convergence ratios for various combinations of γ and $p(x,y)$.*

An important observation is that the functions used in these tests all conform to the sufficient conditions of Theorem 1, most notably that $p(x,y) > 0$ on its domain. It is useful to examine whether these conditions are also necessary, at least for the numerical methods whose behavior we now consider when the condition $p(x,y) > 0$ is violated. The logarithm of the residual norm, as a function of the number of V-cycles, is plotted in Figure 4 for the case $p(x,y) = x - 1/2$, with $\gamma = 1$. As is easily seen, the method does not converge in this case (nor, apparently, does it diverge). Other examples may also be found in which $p(x,y) < 0$ in some neighborhood of the domain, and the numerical methods fail to converge. One such example is given by $p(x,y) = 2\sin(2\pi x)\sin(2\pi y)$.

Figure 5, on the other hand, tells an interesting story. Here the condition $p(x,y) > 0$ is violated by having $p(x,y) \geq 0$ throughout the domain, with equality holding throughout much of the domain. In this case, $p(x,y) = \max\{-x+1/4, 0, x-3/4\}$, and $p(x,y)$ is shown in the left of the figure. The logarithm of the residual is shown in the middle of the figure, plotted against the number of V-cycles. It is seen that the method converges in this case, and in fact, converges with a residual norm ratio that is remarkably stable at 0.201, through 12 V-cycles, bringing the residual norm to 10^{-9}. This conforms to the conditions of Theorem 2. The solution to the problem is shown in the right of the figure. Other functions in which $p(x,y) \geq 0$ within the domain also converge. For example, with $p(x,y) = 2\sin^2(2\pi x)\sin^2(2\pi y)$ convergence is observed with a steady residual norm ratio of 0.108.

Other examples of interest are generated using step functions, and are used to illustrate Theorem 3. This theorem guarantees the existence of weak solutions, rather than classical solutions, but we may still attempt to find explicit solutions

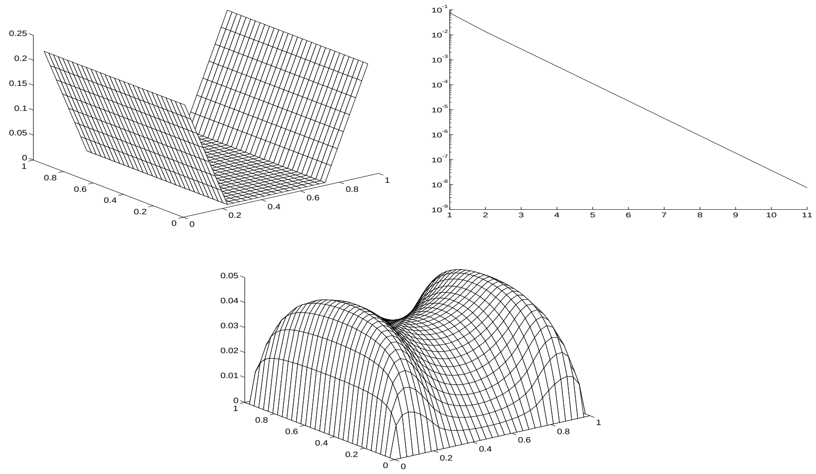

Figure 5: TOP LEFT: *the function* $p(x, y) = \max\{-x+1/4, 0, x-3/4\}$. TOP RIGHT *The logarithm of the residual norm, as a function of the number of V-cycles. The method converges at a remarkably steady ratio in this case.* BOTTOM: *The solution* $u(x, y)$.

numerically. For the one dimensional case we use $p(x) = H(x - 0.5)$, where $H(x)$ is the Heaviside function

$$H(x) = \begin{cases} 0 & \text{if } x < 0 \\ \\ 1 & \text{if } x \geq 0, \end{cases}$$

while for the two-dimensional case we use $p(x, y) = H(x - 0.5)H(y - 0.5)$. In both the one- and two-dimensional cases the numerical method works extrememly well. Solutions and residual norms are displayed in Figure 6. In the one-dimensional case it can be seen that the solution conforms well to our intuition developed in single-variable calculus. Where $p(x) = 0$ the solution appears as a straight line, befitting the solution of Laplace's equation in one dimension. Where $p(x) = 1$ the solution appears to have constant curvature, again conforming to intuition. The same phenomena are present in the two-dimensional case, but are somewhat more difficult to identify because the physical interpretation of $\Delta\phi$ is not precisely the same as it is in the one-dimensional case.

5 Conclusions

Our survey of existence and uniqueness results has shown that the problem

$$\Delta u + p(x)\, u^{-\gamma} = 0 \quad x \in \Omega$$

is guaranteed to have unique solutions under certain conditions, although these solutions will not be known in closed form. The problem arises in certain non-

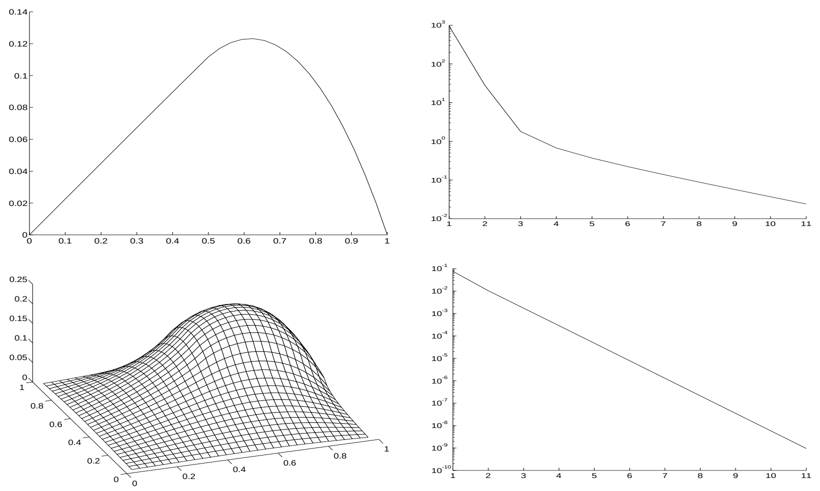

Figure 6: TOP LEFT: *Solution to the one-dimensional problem with* $p(x) = H(x-0.5)$. TOP RIGHT *The logarithm of the residual norm, as a function of the number of V-cycles. The ratio of convergence diminishes after the first few V-cycles.* BOTTOM LEFT: *The solution* $u(x,y)$. *for the two-dimensional problem with* $p(x,y) = H(x-0.5)H(y-0.5)$. BOTTOM RIGHT: *The logarithm of the residual norm for the two-dimensional case, as a function of the number of V-cycles. Convergence occurs with a remarkably steady ratio in this case.*

Newtonian fluids problems, so there is some interest in actually computing solutions. We have shown that for homogeneous Dirichlet boundary conditions on the unit interval and the unit square, multigrid methods provide an efficient means of solution for appropriate choices of $p(x)$.

6 References

[1] Achi Brandt. *Mulitgrid techniques: 1984 guide with application to fluid dynamics.* GMD-Studien Nr. 85. Gesellschaft für Mathematik und Datenverarbeitung, St. Augustin, 1984.

[2] William L. Briggs. *A Multigrid Tutorial.* Society for Industrial and Applied Mathematics, Philadelphia, 1987.

[3] A. J. Callegari and A. Nachman. A nonlinear singular boundary value problem in the theory of pseudoplastic fluids. *SIAM J. Appl. Math*, 30:275–281, 1980.

[4] A. Edelson. Entire solutions of singular elliptic equations. *J. Math. Anal. Appl.*, 139:523–532, 1989.

[5] T. Kusano and A. Swanson. Entire positive solutions of singular semilinear elliptic equations. *Japan J. Math.*, 11, 1985.

[6] A. C. Lazer and P. J. McKenna. On a singular nonlinear elliptic boundary value problem. *Proceedings of the AMS*, 111:721–730, 1991.

[7] A. V. Lair and A. W. Shaker. Entire solution of a singular semilinear elliptic problem. *J.M.A.A.*, to appear.

[8] A. V. Lair and A. W. Shaker. Classical and weak solutions of a singular semilinear elliptic problem. Submitted.

[9] Jan Mandel, Stephen F. McCormick, and R. Bank. Variational multigrid theory. In Stephen F. McCormick, editor, *Multigrid methods*, volume 3 of *Frontiers in applied mathematics*, pages 131–177, Philadelphia, PA, 1987. Society for Industrial and Applied Mathematics.

[10] W. Ni. On the elliptic equation $\delta u + k(x)u^{(n+2)/(n-2)} = 0$, its generalization and application in geometry. *Indiana Univ. Math. J.*, 31:493–525, 1982.

[11] Manuel A. del Pino. *A global estimate of the gradient in a singular elliptic boundary value problem*. Proceedings of the Royal Society of Edinburgh, 122A, 341-352, 1992.

[12] D. H. Sattinger. *Topics in stability snd bifurcation theory*. Springer-Verlag, Berlin, 1973.

[13] A. W. Shaker. On singular semilinear elliptic equations. *J. Math. Anal. and Appl.*, 173:222–228, 1993.

[14] K. Stüben and Ullrich Trottenberg. Multigrid methods: Fundamental algorithms, model problem analysis and applications. In W. Hackbusch and U. Trottenberg, editors, *Multigrid methods, proceedings of a conference held at Köln-Porz, November 23-27, 1981*, volume 960 of *Lecture notes in mathematics*, pages 1–176, Berlin, 1982. Springer-Verlag.

[15] J. S. Wong. On the generalized Emden-Fowler equation. *SIAM Rev.*, **17** (1975), 339-360.